

# Regulation of Electrochemical Oxidation of Glucose by Ionic Strength-Controlled Virtual Area of Nanoporous Platinum Electrode

Jongwon Kim and Sejin Park<sup>†\*</sup>

Department of Chemistry, Chungbuk National University, Cheongju, Chungbuk 361-763, Korea

<sup>†</sup>Basic Science Research Institute, Sungshin Women's University, 249-1 Dongseon-dong, Seongbuk-gu, Seoul 136-742, Korea

(Received June 11, 2007; Accepted July 25, 2007)

**Abstract :** Electrochemical reaction of glucose was regulated by the electrochemically active area of nanoporous platinum, which is controlled by ionic strength. The profile of the oxidation current of glucose vs. ionic strength was identical with that of the electrochemically active area. This result confirms that the nanopores are virtually opened for the electrochemical reaction of glucose when the ionic strength climbs over a specific concentration and implies that the electrochemical reactions on nanoporous electrode surfaces can be controlled by concentration of electrolyte.

**Keywords :** Nanopore, Mesopore, Debye length, Electrical double layer, Glucose.

## 1. Introduction

Since the nanoporous platinum (H<sub>1</sub>-ePt) electrochemically deposited from hexagonal lyotropic liquid crystal (H<sub>1</sub>-LLC) with pore diameter of 2.5 nm was first reported,<sup>1)</sup> the interest on the nanoporous interface between metal and electrolyte has been continuously increased. The state-of-the-art techniques to fabricate nanoporous metal surface are the electrochemical deposition in bulk or electrically induced LLC,<sup>1,2)</sup> dissolution of alloys,<sup>3,4)</sup> and chemical plating on nanoporous membranes.<sup>5)</sup> Variety of metals such as platinum,<sup>1,2)</sup> gold,<sup>5)</sup> and tin<sup>6)</sup> has been fabricated in nanoporous form using those methods. Following the progress in fabrication techniques, the electrochemical phenomena at the interface between nanoporous metal and electrolyte are attracting interest of researchers. The electrochemical reactions of glucose,<sup>7)</sup> hydrogen peroxide,<sup>8)</sup> methanol,<sup>9)</sup> and oxygen<sup>9,10)</sup> were studied on the nanoporous metal electrode surfaces. The application areas proposed in those studies were sensors,<sup>7,8,11,12)</sup> fuel cells<sup>9,10)</sup> and batteries.<sup>6)</sup>

In previous work in our group, it was proposed that the electrochemically active area of the nanoporous electrode surface can be regulated by adjusting the ionic strength of the solution.<sup>13)</sup> That is, the area of the interface between the electrical double layer and the bulk solution phase varies depending on the ionic strength and thus the faradaic reactions occurring across the interface can be critically controlled by electrolyte concentration for nanoporous electrodes. According to Gouy-Chapman theory,<sup>14)</sup> the geometric area enlarged by morphological porosity is not necessarily equivalent to electrochemically active area of the electrode surfaces, which can be described as a function of two variables. One is the pore radius ( $r$ ) and the other is the characteristic thickness of the

double layer, so called Debye length ( $\kappa^{-1}$ ). The  $\kappa^{-1}$  characterizes the spatial decay of potential at electrode-electrolyte interface. The Gouy-Chapman theory states

$$\kappa = (3.29 \times 10^7) z C^*{}^{1/2} \quad (1)$$

where  $C^*$  is the bulk concentration of  $z : z$  electrolyte (in mol L<sup>-1</sup>) and  $\kappa$  is double layer thickness parameter (cm<sup>-1</sup>). The Debye length is an equi-potential line that is far from the electrode surface by  $\kappa^{-1}$ , which decreases as electrolyte concentration increases. When  $\kappa^{-1} < r$ , the equi-potential line is so close to the surface of the pores that the active area should be equivalent to the morphological porosity. On the other hand, when  $\kappa^{-1} > r$ , the pore is so narrow that the electrical double layer extends to outside of the pores and no substantial potential drop occurs inside the pores. Thus, a critical change in the shape of the electric double layer and the decrease of the active surface area take place to the surface of nanoporous electrodes when the diameter of pores falls down to the thickness of the electrical double layer. Fig. 1 shows the schematic diagrams of the shapes of the electrical double layers with different electrolyte concentrations.<sup>13)</sup> A virtual pore closing happens at lower electrolyte concentrations (Fig. 1 (a) and (b)), and a virtual opening of pores occurs at higher electrolyte concentrations. (Fig. 1 (c) and (d)).

It is known that the differential capacitance ( $C_d$ )<sup>15)</sup> can be served as a good experimental indicator to probe the change in effective electrode surface area for nanoporous Pt (pore diameter of 2.5 nm)<sup>1)</sup> and NaF.<sup>14)</sup> It was reported that the  $C_d$ 's of nanoporous Pt electrode surfaces rise precipitously in electrolyte concentrations higher than  $1 \times 10^{-2}$  M, where  $\kappa^{-1}$  is theoretically equal to  $r$  (1.25 nm).<sup>13)</sup> It was proposed that the control of faradaic current density for kinetic-controlled reaction by altering supporting electrolyte concentration could be realized, and the electrochemical reduction of diox-

\*E-mail: yyepi@sungshin.ac.kr

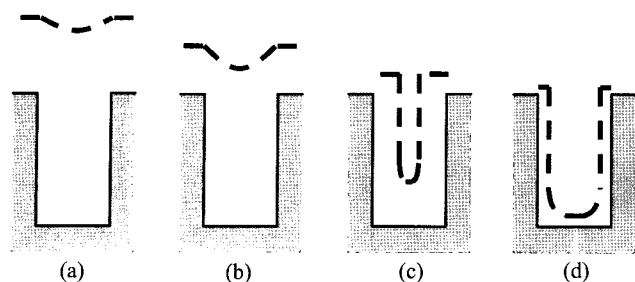


Fig. 1. Schematic diagrams of the shapes of the electrical double layers and nanopores according to the change of the electrolyte concentrations (from previous report<sup>13</sup>). (a) 1 mM, (b) 10 mM, (c) 100 mM, and (d) 1000 mM.

xygen was demonstrated as an application example of the unique behavior on the nanoporous Pt electrodes.<sup>13</sup> In the present study, this unique phenomenon is demonstrated again for the oxidation of glucose. The electrochemical oxidation of glucose is interesting issue for the development of nonenzymatic glucose sensors. The oxidation of glucose is kinetically more sluggish than the reduction of dioxygen, therefore we expect that the oxidation behavior of glucose on nanoporous Pt surfaces with various electrolyte concentrations clearly demonstrates the virtual pore closing/opening phenomenon. Furthermore, it was reported that the nanoporous Pt electrode surfaces selectively enhance the oxidation of glucose and this phenomenon originates from the nanopore structure on the Pt surfaces.<sup>7</sup> Thus, the electrochemical behavior of glucose oxidation depending on ionic strength is worth of investigation to further understand the selective oxidation of glucose on nanoporous Pt surfaces.

## 2. Experimental section

### 2.1 Reagents

Octaethylene glycol monohexadecyl ether  $C_{16}EO_8$  (Fluka), hydrogen hexachloroplatinate hydrate (Aldrich), sulfuric acid, D-(+)-glucose (Sigma), sodium fluoride, and sulfuric acid were used without purification.

### 2.2 Instruments

Electrochemical experiments were performed using an electrochemical analyzer (Model CH660, CH Instruments Inc., Austin, TX 78733). A Ag/AgCl (3 M KCl) or Hg/Hg<sub>2</sub>SO<sub>4</sub> (sat'd) and a platinum wire were used as reference and counter electrodes, respectively. A gold rod electrode (0.0079 cm<sup>2</sup>) was used as a substrate electrode for the H<sub>1</sub>-ePt film deposition. Small angle X-ray diffraction was measured using a small angle X-ray scattering unit fitted with general area detector diffraction (Bruker, Germany).

### 2.3 Preparation of LLC and electrodeposition of H<sub>1</sub>-ePt

$C_{16}EO_8$  (0.42 g), distilled water (0.29 g), and hydrogen hexachloroplatinate hydrate (0.29 g) were mixed, and the temperature was raised to 80°C, where the mixture became transparent and homogeneous. Au electrodes were then

inserted into the homogeneous mixture, and temperature was lowered to room temperature. At this stage, the mixture became a highly viscous LLC material. Platinum deposition was carried out at constant potential (-0.06 V vs. Ag/AgCl). The resulting nanoporous platinum electrode was placed in distilled water for 1 hr to extract the residual  $C_{16}EO_8$ , and the extraction procedure was repeated 3-4 times. The electrode was then electrochemically cleaned by cycling potential between +1.2 and -0.22 V vs. Ag/AgCl in 1 M sulfuric acid until reproducible cyclic voltammograms were obtained.

### 2.4 Electrochemical experiments

All electrochemical measurements were done in a 3-electrode system. The surface areas of the Pt electrodes were determined by measuring the areas under the hydrogen adsorption/desorption peaks of the cyclic voltammograms (scan rate, 0.2 V sec<sup>-1</sup>) in 1.0 M sulfuric acid solution. A conversion factor of 210  $\mu\text{C cm}^{-2}$  was used to determine the electrode area.<sup>16</sup> The electrochemical oxidation of glucose on the H<sub>1</sub>-ePt electrode was observed in N<sub>2</sub>-purged 5 mM glucose solution containing sodium fluoride solutions with a series of concentrations (0.001, 0.01, 0.05, 0.2, 1.0 M) in a temperature-controlled electrochemical cell (37.2 ± 0.2°C). Chronoamperometric curves were obtained for 100 s in a quiescent solution after applying -0.04 V vs Hg/Hg<sub>2</sub>SO<sub>4</sub>.

## 3. Results and discussion

H<sub>1</sub>-ePt films were electroplated on Au electrode surfaces in the H<sub>1</sub>-LLC at -0.06 V vs. Ag/AgCl. H<sub>1</sub>-ePt electrode surfaces as electroplated exhibit shiny dark gray colors, which indicate their excellent flatness of the surface in the scale of visible-light wavelength. Although the H<sub>1</sub>-ePt electrode surface appears to be flat in macroscopic view, it has a very large surface area due to the nanoporous surface structure. Fig. 2 shows the cyclic voltammogram of H<sub>1</sub>-ePt in 1 M H<sub>2</sub>SO<sub>4</sub> solution. The specific surface area of the ePt-H<sub>1</sub> can be measured by integrating the area under the hydrogen adsorption

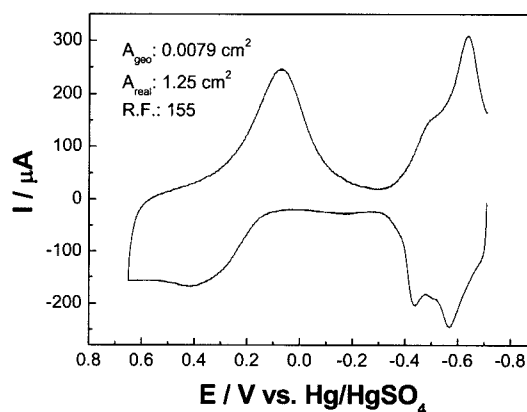


Fig. 2. Cyclic voltammogram of H<sub>1</sub>-ePt an electrode surface in 1.0 M H<sub>2</sub>SO<sub>4</sub> solution with scan rate of 0.2 V/s. H<sub>1</sub>-ePt was deposited electrochemically by passing 25 mC of charge on a Au electrode surface.

peaks. The surface roughness of electroplated the H<sub>1</sub>-ePt film was calculated to be 155. The shiny surface color and the high roughness factor of the electroplated H<sub>1</sub>-ePt films imply the existence of nanoporous structures on the surfaces. In small angle X-ray scattering pattern, a single X-ray diffraction peak appeared at 1.68Å (2θ) corresponding to a pore-pore distance of 6.1 nm (for a hexagonal structure), which is a similar value to that found previously by Gollas et al. (5.9 nm).<sup>17)</sup>

Fig. 3 shows the oxidative currents of 5 mM glucose as a function of time on H<sub>1</sub>-ePt electrodes in N<sub>2</sub>-purged solutions containing NaF concentrations of 0.001, 0.010, 0.050, 0.20, and 1.0 M. The chronoamperometric curves exhibit fast decrease in 20 s and reach quasi-steady current levels after 40 s. In the case of low NaF concentrations (0.001 and 0.01 M), the magnitude of quasi-steady oxidative currents are negligible compared to those obtained in pure NaF solutions without glucose. On the other hand, steep increase in the oxidative signal occurs as the electrolyte concentration passes over 0.05 M. Fig. 4 shows the dependence of oxidative signal (*I<sub>a</sub>*),

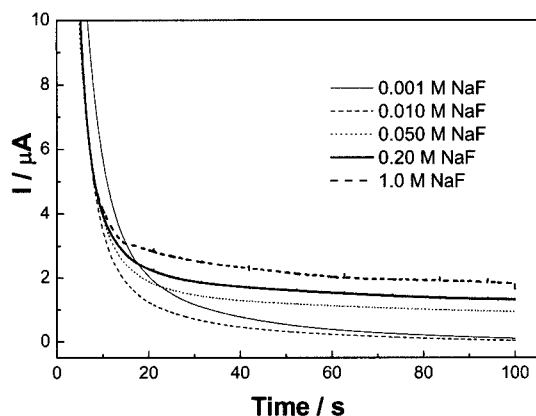


Fig. 3. *I-t* curves measured in N<sub>2</sub>-purged 5 mM glucose solutions with various NaF concentrations (0.001, 0.010, 0.050, 0.201, 1.0 M) at -0.04 V vs Hg/Hg<sub>2</sub>SO<sub>4</sub>. Background correction was performed by subtracting currents measured in NaF solutions without glucose (blank solution). Measurements of glucose oxidation currents were performed after electrochemical cleaning of the H<sub>1</sub>-ePt films in 1 M H<sub>2</sub>SO<sub>4</sub> solution.

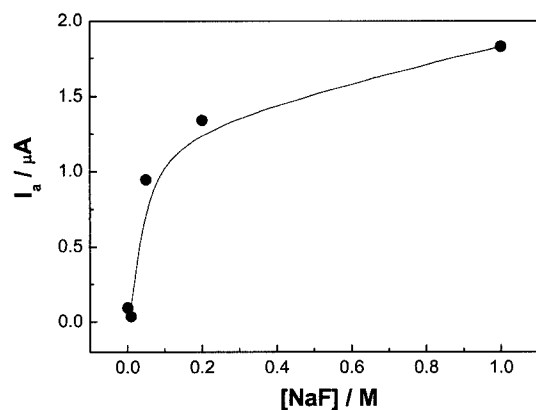


Fig. 4. The effect of ionic strength on the glucose oxidation current. The currents were sampled at 100 s of the corresponding curves of Fig. 3.

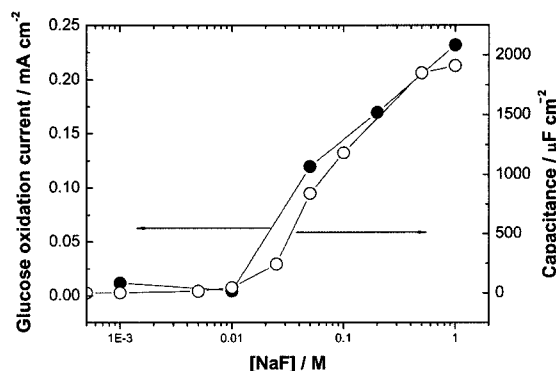


Fig. 5. Dependence of differential capacitances (open circles, from data of previous report<sup>13)</sup>) and glucose oxidation current density (filled circle, redrawn from Fig. 4) on electrolyte concentrations.

measured at 100 s in chronoamperometric curves in Fig. 3, on the electrolyte concentration. Abrupt increase of oxidative signal is shown near an electrolyte concentration of 0.05 M, and the oxidative current becomes less dependent on the electrolyte concentrations above 0.2 M. This indicates that the Debye length in the electrical double layer ( $\kappa^{-1}$ ) is larger than the pore radius (*r*) when the electrolyte concentration is smaller than 0.05 M. Thus the equi-potential line cannot be formed inside the nanopores, which results in a virtual pore closing. (Refer to Fig. 1(a)) At higher electrolyte concentrations, on the other hand,  $\kappa^{-1}$  values decrease as expected in equation (1) and become smaller than the pore diameter. Now the equi-potential line can penetrate inside the nanopores and as a result glucose oxidation occurs on the surface of the inside pores (pore opening).

The results presented here coincide well with those previously reported that the differential capacitance increases dramatically between the electrolyte concentrations of 0.01 and 0.1 M.<sup>13)</sup> The open circles in Fig. 5 show a dependence of differential capacitance values on electrolyte concentrations (from data of previous report<sup>13)</sup>) measured on a H<sub>1</sub>-ePt electrode surface with a roughness factor of 158 which is close to the roughness factor for H<sub>1</sub>-ePt electrode investigated in this study. The oxidative current densities of glucose vs. the NaF concentrations (log scale, redrawn from Fig. 4 for comparison purpose) are shown as filled circles in Fig. 5. There is a similar tendency between the differential capacitance and glucose oxidation currents. Both of the values remain almost at background levels up to the electrolyte concentrations less than 0.01 M, thereafter start to increase linearly with the log electrolyte concentrations. These results demonstrate the regulation of faradaic currents from glucose oxidation by adjusting the electrolyte concentrations.

#### 4. Conclusions

The electrochemical oxidation of glucose occurs across the equi-potential line being far from the electrode surface by Debye length. A virtual nanopore opening/closing by controlling electrolyte concentrations was demonstrated for glucose oxidation

and compared to our previous report for dioxygen reduction. These results suggest that the electrochemical event at the interface of nanoporous surface and solution might be seriously sensitive to the ionic strength of the solution, and the electrolyte concentration could be significant variable for the electrochemical reaction.

### Acknowledgement

“This work was supported by the Korea Research Foundation Grant funded by Korea Government (MOEHRD, Basic Research Promotion Fund)” (KRF-2005-075-C00021)

### References

1. G. S. Attard, P. N. Bartlett, N. R. B. Coleman, J. M. Elliott, J. R. Owen, and J. H. Wang, “Mesoporous platinum films from lyotropic liquid crystalline phases” *Science*, **278**, 838 (1997).
2. K.-S. Choi, E. W. McFarland, and G. D. Stucky, “Electrocatalytic properties of thin mesoporous platinum films synthesized utilizing potential-controlled surfactant assembly” *Adv. Mater.*, **15**, 2018 (2003).
3. Y. Ding, and J. Erlebacher, “Nanoporous metals with controlled multimodal pore size distribution” *J. Am. Chem. Soc.*, **125**, 7772 (2003).
4. C. Ji, and P. C. Searson, “Synthesis and characterization of nanoporous gold nanowires” *J. Phys. Chem. B*, **107**, 4494 (2003).
5. K. B. Jirage, J. C. Hulteen, and C. R. Martin, “Effect of thiol chemisorption on the transport properties of gold nanotubule membranes” *Anal. Chem.*, **71**, 4913 (1999).
6. A. H. Whitehead, J. M. Elliott, J. R. Owen, and G. S. Attard, “Electrodeposition of mesoporous tin films” *Chem. Commun.*, 331 (1999).
7. S. Park, T. D. Chung, and H. C. Kim, “Nonenzymatic glucose detection using mesoporous platinum” *Anal. Chem.*, **75**, 3046 (2003).
8. S. A. G. Evans, J. M. Elliott, L. M. Andrews, P. N. Bartlett, P. J. Doyle, and G. Denuault, “Detection of hydrogen peroxide at mesoporous platinum microelectrodes” *Anal. Chem.*, **74**, 1322 (2002).
9. A. Kucernak, and J. Jiang, “Mesoporous platinum as a catalyst for oxygen electroreduction and methanol electrooxidation” *Chem. Eng. J.*, **93**, 81 (2003).
10. P. R. Birkin, J. M. Elliott, and Y. E. Watson, “Electrochemical reduction of oxygen on mesoporous platinum microelectrodes” *Chem. Commun.*, 1693 (2000).
11. P. N. Bartlett, and S. Guerin, “A micromachined calorimetric gas sensor: an application of electrodeposited nanostructured palladium for the detection of combustible gases” *Anal. Chem.*, **75**, 126 (2003).
12. S. Park, H. Boo, Y. Kim, J.-H. Han, H. C. Kim, and T. D. Chung, “pH-sensitive solid-state electrode based on electrodeposited nanoporous platinum” *Anal. Chem.*, **77**, 7695 (2005).
13. H. Boo, S. Park, B. Ku, Y. Kim, J. H. Park, H. C. Kim, and T. D. Chung, “Ionic strength-controlled virtual area of mesoporous platinum electrode” *J. Am. Chem. Soc.*, **126**, 4524 (2004).
14. A. J. Bard, and L. R. Faulkner, “Electrochemical methods: Fundamentals and Applications”, Wiley, New York (2001).
15. J. O. M. Bockris, and S. U. M. Khan, “Surface electrochemistry”, 321, Plenum, New York (1993).
16. S. Trasatti, and O. A. Petrii, “Real surface-area measurements in electrochemistry” *J. Electroanal. Chem.*, **327**, 353 (1992).
17. B. Gollas, J. M. Elliott, and P. N. Bartlett, “Electrodeposition and properties of nanostructured platinum films studied by quartz crystal impedance measurements at 10 MHz” *Electrochim. Acta*, **45**, 3711 (2000).